Journal of Alloys and Compounds 489 (2010) 332–335

Contents lists available at ScienceDirect

Journal of Alloys and Compounds

journal homepage: www.elsevier.com/locate/jallcom

Observation of two separate charge density wave transitions in Gd_2Te_5 via transmission electron microscopy and high-resolution X-ray diffraction

K.Y. Shin[a,b], N. Ru[a,b], I.R. Fisher[a,b,*], C.L. Condron[c,1], M.F. Toney[c], Y.Q. Wu[d], M.J. Kramer[d]

[a] Geballe Laboratory for Advanced Materials and Department of Applied Physics, Stanford University, Stanford, CA 94305, USA
[b] Stanford Institute for Materials and Energy Sciences, SLAC National Accelerator Laboratory,2575 Sand Hill Road, Menlo Park, California 94025, USA
[c] Stanford Synchrotron Radiation Lightsource, SLAC National Accelerator Laboratory, 2575 Sand Hill Road, Menlo Park, California 94025, USA
[d] Ames Laboratory and Department of Materials Science and Engineering, Iowa State University, Ames, IA 50011, USA

ARTICLE INFO

Article history:
Received 7 September 2009
Received in revised form
19 September 2009
Accepted 24 September 2009
Available online 4 October 2009

Keywords:
Charge density wave
Intermetallics
Transmission electron microscopy
X-ray diffraction

ABSTRACT

Gd_2Te_5 is a layered material consisting of alternating single and double square planar Te sheets. At room temperature the material hosts a complex lattice modulation characterized by multiple in-plane wavevectors. Diffraction measurements performed via transmission electron microscopy and high-resolution X-ray scattering reveal two distinct transitions at $T_{c1} = 410(3)$ and $T_{c2} = 532(3)$ K, associated with an on-axis incommensurate lattice modulation and an off-axis commensurate lattice modulation respectively. Our results show that the two lattice modulations are separate in origin but that there is some coupling between them.

1. Introduction

Charge density waves (CDWs) are a familiar concept in condensed matter physics [1]. The basic premise is that a large electronic susceptibility at finite wavevector q, such as can be generated by Fermi surface nesting in low dimensional materials, can lead to a coupled electronic/lattice instability if the electron–phonon coupling is strong enough. In recent years there has been renewed interest in this broken symmetry state for quasi-two-dimensional (2d) materials, motivated in part by the desire to better understand charge-ordered states in strongly correlated systems such as the cuprate superconductors [2]. In this regard, the rare earth (R) tellurides RTe_2 and RTe_3, based on single and double square Te planes respectively, are especially revealing, and have attracted particular interest given the combination of their simple electronic structure [3–5], simple lattice modulation [6–8], easy "tunability" (both in terms of band filling [9,10] and also chemical pressure [11]), and finally the large magnitude of their CDW gap [12]. This renders these materials appropriate for several powerful and complementary probes of the electronic and physical structure [13–16]. Several studies have established these as prototypical nesting-driven CDW systems, with CDW wave vectors determined by well-defined peaks in the Lindhard susceptibility [2,4,17], although questions remain about the role played by a possible incipient lattice instability [18].

Recently, the closely related family of compounds R_2Te_5 have also been shown to host CDW modulations [19–21]. Based on alternating single and double Te planes, interleaved by corrugated RTe layers [22], this new family of compounds is essentially a hybrid of the simpler RTe_2 and RTe_3 compounds. This material raises the very interesting question of how CDW formation on the different Te planes coexists, or even competes. To begin to address this question, we consider the representative compound Gd_2Te_5. Our initial observation revealed two distinct sets of modulation wavevectors at room temperature for this material, one of which is incommensurate ($q_0 \sim 0.69c^*$), and the other of which is fully commensurate ($q_1 = 5/12a^* + 1/12c^*$, $q_2 = 1/12a^* + 5/12c^*$). Both of these can be correlated with separate contributions to the Lindhard susceptibility, indicating that the CDWs originate independently on the single and double Te planes [19]. In this regard, Gd_2Te_5 can be considered a quasi-2d analog of the well-known quasi-1d material $NbSe_3$. In the case of $NbSe_3$, successive CDW transitions at 59 and 145 K [23] have been associated separately with inequivalent and nominally non-interacting prismatic chains [24–27]. In this short paper, we establish via Transmission Electron Microscopy (TEM) and high-resolution X-ray diffraction that the two sets of modulation wave vectors observed in Gd_2Te_5 undergo separate phase transitions as a function of temperature at $T_{c1} = 410(3)$ and $T_{c2} = 532(3)$ K. This

* Corresponding author. Tel.: +1 650 723 5821; fax: +1 650 725 2189.
E-mail address: irfisher@stanford.edu (I.R. Fisher).
[1] Present address: Rapiscan Systems, 520 Almanor Ave., Sunnyvale, CA 04085, United States.

0925-8388/$ – see front matter © 2009 Elsevier B.V. All rights reserved.
doi:10.1016/j.jallcom.2009.09.154

result confirms the separate origin of the two lattice modulations, and delineates ranges of temperature over which the interplay between the two CDW states can be investigated in greater detail. The substantially higher CDW transition temperatures found in Gd_2Te_5 than for the 1d analog $NbSe_3$ may indicate a greater potential for observing interactions between the two CDW condensates.

2. Experimental methods

Single crystals of Gd_2Te_5 were grown by slowly cooling a binary melt, as described previously [19]. TEM diffraction images were taken at various temperatures along the (0 1 0) zone axis, i.e. perpendicular to the Te planes. The samples were ion-milled using a liquid nitrogen cooling stage, and selected area diffraction patterns (SADPs) were taken using a Philips CM 30 operating at 300 keV with a Gatan double tilt heating stage for temperatures up to 540 K, utilizing double copper washers to improve thermal contact. The equipment was optimized at the nominal camera length 900 mm and images were taken at varied exposure stops to obtain enough sensitivity for the weak superlattice reflections. Real space images showed very few macroscopic defects, which were easily avoided.

High-resolution X-ray diffraction measurements were performed at the Stanford Synchrotron Radiation Lightsource (SSRL) on Beam Lines 11-3 and 7-2. Samples were glued on the surface of a metallic sample stage using silver epoxy and the temperature was actively controlled by an Anton-Paar furnace up to 550 K. The samples were kept in a helium gas flow during the entire experiment in order to minimize oxidation. Measurements were carried out in a reflection geometry for photon energies 9.35 keV and 12.70 keV. A Ge(1 1 1) crystal analyzer or either 1 mrad or 2 mrad slits was selected depending on the measurement. Bragg peaks and the CDW satellite peaks over a wide range of ($h\,k\,l$) were carefully inspected in order to select regions of minimal structural defects. Samples had to be realigned at each temperature due to the thermal expansion of the sample stage, and the Bragg peaks near to the satellite peaks were centered at the maximum intensities. CDW peaks were sharply peaked (inset to Fig. 3(a)) and we obtain a lower bound for the CDW correlation length of ~0.5 μm in the *ac* plane and ~0.05 μm along the *b*-axis for both on- and off-axis CDWs.

3. Results and discussion

SADPs taken at room temperature both before and after heating to 536 K are shown in Fig. 1, where the modulation wave vectors q_0, q_1 and q_2 are labeled around ($h\,0\,l$) = (1 0 1). Fig. 1(a) shows that the initial diffraction pattern before heating is actually a mirror image of the satellite peaks previously observed in Ref. [19] and we label the diffraction peaks accordingly $q_1' = -5/12a* + 1/12c*$ and $q_2' = -1/12a* + 5/12c*$. After heating and subsequent cooling to room temperature (Fig. 1(b)), the diffraction pattern shows weak circular streaks, caused by irreversible surface recrystallization at high temperatures. The diffraction pattern has also suffered a mirror reflection about the c^*axis, ascribed to a reversal of the CDW domain orientation.

Representative SADPs taken at 343 K, 446 K and 536 K are shown in Fig. 2(a–c) respectively. The images were taken sequentially while warming from room temperature. Both domains of the commensurate lattice modulation (i.e. q_1 and q_2 oriented to the right and to the left) were observed for temperatures above 313 K (see for example Fig. 2(a)). Compared to the commensurate off-axis modulation peaks, the incommensurate CDW along the c^* axis did not show a similar effect, due to the inequivalence of the *a* and *c* axes.

The diffraction intensities for q_0 were tremendously reduced by 343 K (green arrows in Fig. 2(a)) and had disappeared by 446 K (Fig. 2(b)). In contrast, the intensities for the off-axis superlattice peaks remained strong until much higher temperatures, eventually almost vanishing at the highest temperatures (536 K, Fig. 2(c)).

The CDW transitions were investigated in greater detail via high-resolution X-ray diffraction. The temperature dependence of the incommensurate CDW peaks for ($h\,k\,l$) = (3 38 1−q_0), (5 38 1−q_0) and (4 39 q_0) is shown in Fig. 3. A rapid increase in FWHM above the resolution limit (shown in Fig. 3(a) for the specific peak (4 39 q_0) in the *ac* plane) signals a CDW transition at T_{c1} = 410(3) K, consistent with TEM data described above. The square root of the integrated intensity, proportional to the order parameter for weakly coupled systems, is shown in Fig. 3(b) for all three peaks, together with the

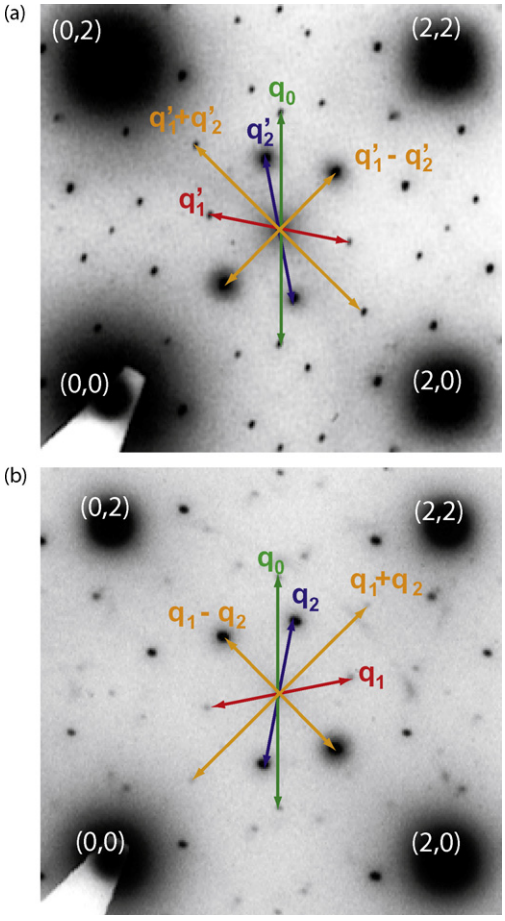

Fig. 1. Selected area TEM diffraction pattern in ($h\,0\,l$) plane at room temperature (a) before and (b) after heating to 536 K. Bragg peaks are labeled according to ($h\,l$). CDW wave vectors are labeled as described in the main text.

mean field BCS curve drawn for T_{c1} = 410 K. Data have been normalized to the BCS curve at 300 K. Residual scattering intensity above T_{c1}, ascribed to fluctuations due to the large FWHM we observe, was observed up to 463 K, above which the satellite peaks became too broad to be distinguished from background.

The absolute value of q_0 changes with temperature, increasing by approximately 1.5% from T_{c1} to room temperature (Fig. 3(c)), and indicating a fully incommensurate CDW. Above T_{c1}, q_0 does not appear to vary as strongly with temperature, but the accuracy of the measurement was limited by the significant broadening of the CDW peak.

The incommensurate CDW transition is also apparent in the lattice parameters (Fig. 3(d)). Above T_{c1}, there is only a small difference (approximately 0.15%) in the in-plane lattice parameters *a* and *c*. On cooling below T_{c1}, there is a marked change in the thermal expansion coefficients, with the *a*-axis lattice parameter decreasing more rapidly with reducing temperature, while the *c*-axis lattice parameter actually increases with reducing temperature, at least in the range from 410 down to 300 K. By room temperature, the *c*-axis lattice parameter is fully 0.60% larger than the *a*-axis. A similar "stretching" of the *c*-axis upon CDW formation was also observed for the equivalent unidirectional incommensurate CDW in the bilayer compound $TbTe_3$ [11].

The temperature dependence of the off-axis commensurate superlattice diffraction peaks was also measured. Data were collected for many peaks and representative measurements for five specific wavevectors are shown in Fig. 4. The diffraction intensities for (4(1/12), 41, (5/12)), (3(8/12), 41, (4/12)), (4(5/12), 44,

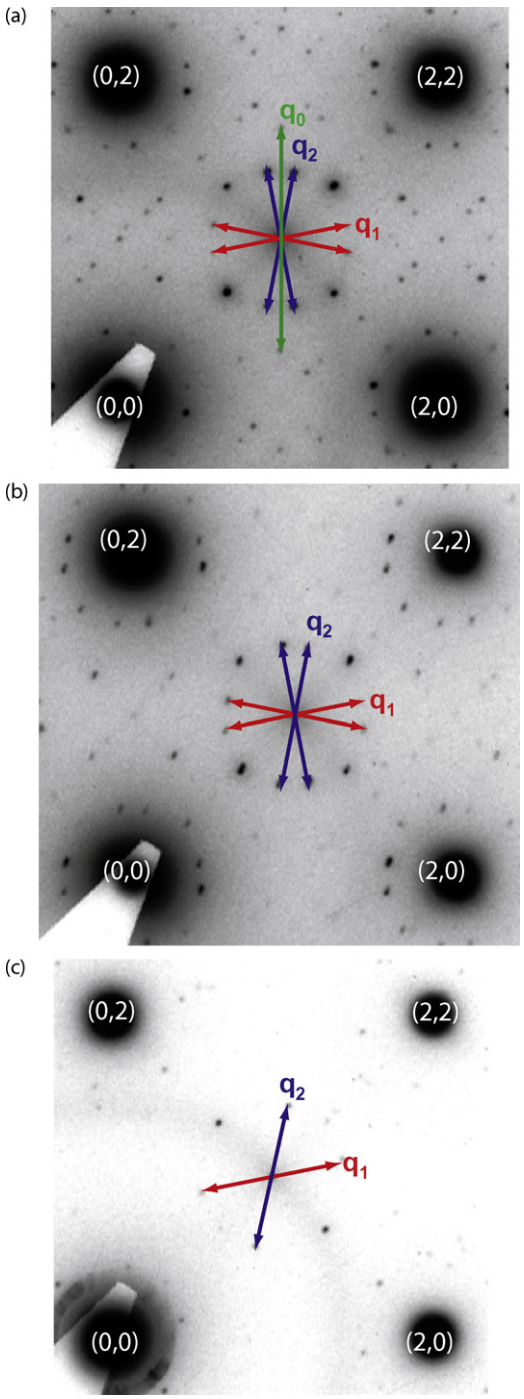

Fig. 2. SADPs at (a) 343 K (b) 446 K and (c) 536 K. Bragg peaks are labeled according to (h l). Wave vectors are labeled as described in the main text. The incommensurate CDW with $q_0 \sim 0.69c^*$ has disappeared by 446 K, suggestive of a CDW transition below this temperature.

(1/12)) and (3(3/12), 39, (3/12)) decreased upon heating and almost disappeared at 533 K (Fig. 4 (a)), suggestive of a phase transition. Oxidation at these elevated temperatures, even in the flowing He atmosphere, meant that data had to be collected rapidly. Consequently, measurements of the FWHM were limited to temperatures below 533 K and, in contrast to the on-axis CDW described above, it was difficult to systematically determine a sharp increase of the peak width associated with the ultimate transition. However, comparison of the temperature dependence of the square roots of the integrated intensities of (4(1/12), 41, (5/12)) and (3(8/12), 41,

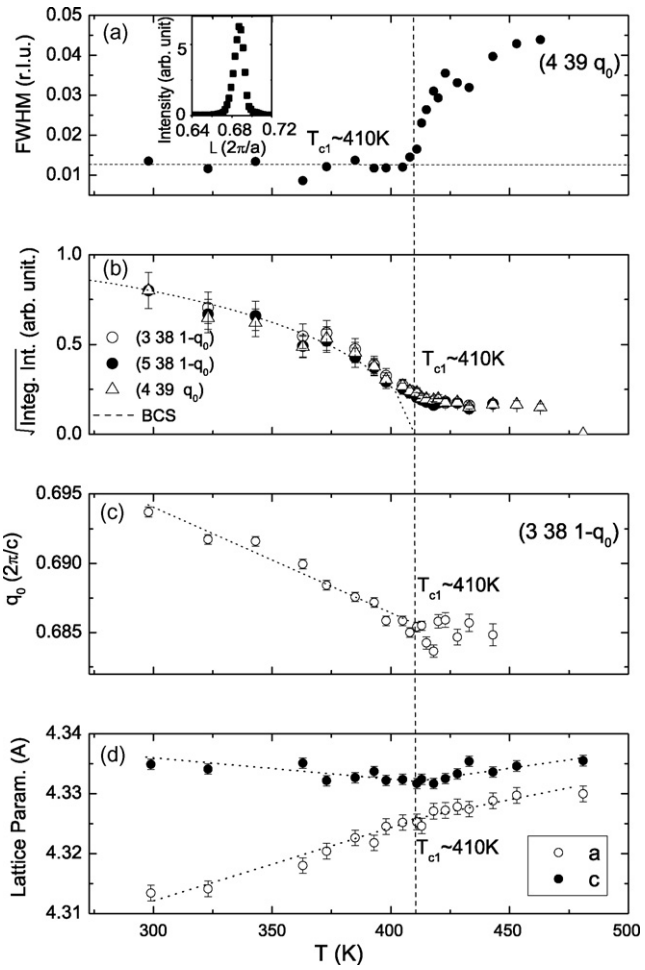

Fig. 3. Temperature dependence of the on-axis incommensurate CDW state. (a) FWHM of the CDW peak at (4 39 q_0) in the ac plane. The sudden increase in FWHM at T_{c1} = 410(3) K indicates a CDW phase transition. Inset shows a representative L scan at 300 K. (b) Square root of the integrated intensity for peaks at (3 38 1−q_0), (5 38 1−q_0) and (4 39 q_0), normalized to the BCS curve at 300 K. (c) CDW wave vector q_0 as a function of temperature measured from the CDW peak at (3 38 1−q_0). (d) In-plane lattice parameters a and c as a function of temperature. The dashed vertical line for all panels indicates the nominal transition temperature T_{c1} = 410 K. r. l. u. refers to reciprocal lattice units.

(4/12)) and the 4th roots of the integrated intensities of (4(5/12), 44, (1/12)) and (3(3/12), 39, (3/12)) with the classical BCS order parameter (Fig. 4(b)) allows an estimate of T_{c2} = 532(3) K for these peaks, in reasonable agreement with the trend observed in TEM. This comparison, which is justified empirically by its success in condensing data for several diffraction peaks on to a single curve, implies that the satellite peaks at (4(1/12), 41, (5/12)) and (3(8/12), 41, (4/12)), corresponding to q_2 and q_2-q_1 respectively are from the fundamental, whereas peaks at (4(5/12), 44, (1/12)), corresponding to q_1 and (3(3/12), 39, (3/12)), corresponding to q_2-2q_1 are second harmonics, and hence that the fundamental wavevectors associated with the off-axis CDW are actually $q_2 = 1/12a^* + 5/12c^*$ and $q_2-q_1 = -4/12a^* + 4/12c^*$. This assignation might be consistent with the relative intensities of the superlattice peaks seen in Fig. 1, but it is not clear that this is the only interpretation for such a fully commensurate lattice modulation. Indeed, the observation of multiple harmonics is perhaps more indicative of a structural phase transition than a CDW *per se*. Regardless of the description of the lattice modulation, which is clearly more complex for the commensurate off-axis case than for the incommensurate on-axis case, the important observation is that the two lattice modulations occur at very different temperatures and are therefore separate in origin.

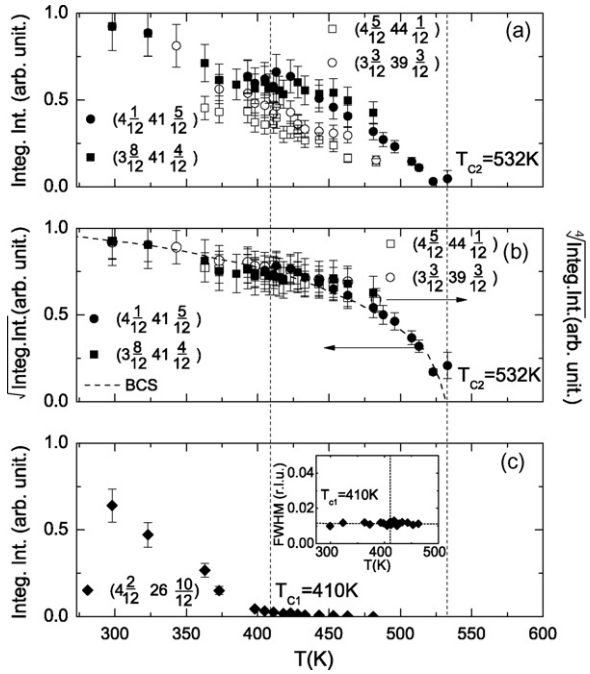

Fig. 4. Temperature dependence of the off-axis commensurate CDW state. (a) Integrated intensities of CDW peaks at (4(1/12), 41, (5/12)), (3(8/12), 41, (4/12)), (4(5/12), 44, (1/12)) and (3(3/12), 39, (3/12)). (b) Square roots of the integrated intensities of (4(1/12), 41, (5/12)) and (3(8/12), 41, (4/12)) (left axis) and 4th roots of the integrated intensities of (4(5/12), 44, (1/12)) and (3(3/12), 39, (3/12)) (right axis). (c) Integrated intensity of the CDW peak at (4(2/12), 26, (10/12)). Inset shows FWHM of the CDW peak at (4(2/12), 26, (10/12)) in the *ac* plane. The intensity decreases significantly at $T \sim T_{c1}$, suggestive of interaction between the on- and off-axis CDWs. The BCS order parameter is shown by a dashed line in panel (b), and vertical dashed lines indicate T_{c1} = 410 K and T_{c2} = 532 K.

ARPES measurements on the single layer RTe_2 compounds [17] indicate a consistently higher maximum CDW gap than the RTe_3 bilayer analogs [12,13]. Although our data do not permit a structural refinement, we have previously argued based on contributions to the Lindhard susceptibility that the off-axis lattice modulation in Gd_2Te_5 is associated primarily with the single Te planes [19]. If this is indeed the case then one might anticipate by analogy with the bilayer compound that the off-axis modulation would have a larger CDW gap, consistent with our observation of a higher critical temperature than for the incommensurate on-axis lattice modulation.

Finally we turn to the question of interaction between the two lattice modulations. Inspection of the data in Fig. 4(a) and (b) indicates that the intensity of the commensurate superlattice reflections might be slightly affected at the onset of the incommensurate on-axis CDW at T_{c1}, but this effect is clearly at the limit of our resolution for these peaks. However, other commensurate CDW peaks exhibit a somewhat stronger effect. For example, the strongest suppression of the reflections for the commensurate superlattice at T_{c1} occurred for the CDW peak at (4(2/12), 26, (10/12)), where the intensity was suppressed almost to zero without increase in the FWHM up to much higher temperatures (Fig. 4(c) and the inset therein). This behavior could not be accounted for by any order of harmonic generation, and suggests a non-trivial coupling of the commensurate and incommensurate CDW order parameters. It will clearly require further experiments to elucidate the nature of this coupling, and the extent to which it affects the underlying electronic structure.

4. Summary

In summary, we have established that the on-axis incommensurate and off-axis commensurate lattice modulations in the novel alternating single and double layer compound Gd_2Te_5 occur at different critical temperatures, and hence are separate in origin. The on-axis incommensurate lattice modulation bears all the hallmarks of a simple CDW transition with T_{c1} = 410(3) K, and is in many ways similar to that found in the closely related bilayer compounds RTe_3. The more complex lattice modulation associated with the off-axis commensurate wavevector has a higher critical temperature, T_{c2} = 532(3) K. These results add weight to the consideration of Gd_2Te_5 as a hybrid of the simpler single and double layer compounds $GdTe_2$ and $GdTe_3$, and delineate regions of temperature over which the interplay between the two lattice modulations can be investigated.

Acknowledgements

This work is supported by the DOE, Office of Basic Energy Sciences, under Contract No. DE-AC02-76SF00515. Efforts at the Ames Laboratory were supported by the DOE under Contract No. DE-AC02-07CH11358. KYS was partly supported by the HS Lee Foundation in South Korea. Portions of this research were carried out at the Stanford Synchrotron Radiation Lightsource (SSRL), a national user facility operated by Stanford University on behalf of the US Department of Energy, Office of Basic Energy Sciences.

References

[1] G. Gruner, Density Waves in Solids, Perseus publishing, 1994.
[2] H. Yao, J.A. Robertson, E.-A. Kim, S.A. Kivelson, Phys. Rev. B 74 (2006) 245126.
[3] A. Kikuchi, J. Phys. Soc. Jpn. 67 (1998) 1308.
[4] J. Laverock, S.B. Dugdale, Zs. Major, M.A. Alam, N. Ru, I.R. Fisher, G. Santi, E. Bruno, Phys. Rev. B 71 (2005) 085114.
[5] J.H. Shim, J.S. Kang, B.I. Min, Phys. Rev. Lett. 93 (2004) 156406.
[6] A. Fang, N. Ru, I.R. Fisher, A. Kapitulnik, Phys. Rev. Lett. 99 (2007) 046401.
[7] C. Malliakas, S.J.L. Billinge, H.J. Kim, M.G. Kanatzidis, J. Am. Chem. Soc. 127 (2005) 6510.
[8] H.J. Kim, C.D. Malliakas, A.T. Tomi, S.H. Tessmer, M.G. Kanatzidis, S.J.L. Billinge, Phys. Rev. Lett. 96 (2006) 226401.
[9] E. DiMasi, M.C. Aronson, J.F. Mansfield, B. Foran, S. LeePhys, Rev. B 52 (1995) 14516.
[10] E. DiMasi, B. Foran, M.C. Aronson, S. Lee, Phys. Rev. B 54 (1996) 13587.
[11] N. Ru, C.L. Condron, G.Y. Margulis, K.Y. Shin, J. Laverock, S.B. Dugdale, M.F. Toney, I.R. Fisher, Phys. Rev. B 77 (2008) 035114.
[12] V. Brouet, W.L. Yang, X.J. Zhou, Z. Hussain, R.G. Moore, R. He, D.H. Lu, Z.X. Shen, J. Laverock, S.B. Dugdale, N. Ru, I.R. Fisher, Phys. Rev. B 77 (2008) 235104.
[13] V. Brouet, W.L. Yang, X.J. Zhou, Z. Hussain, N. Ru, K.Y. Shin, I.R. Fisher, Z.X. Shen, Phys. Rev. Lett. 93 (2004) 126405.
[14] G.-H. Gweon, J.D. Denlinger, J.A. Clack, J.W. Allen, C.G. Olson, E. DiMasi, M.C. Aronson, B. Foran, S. Lee, Phys. Rev. Lett. 81 (1998) 886.
[15] D.R. Garcia, G.-H. Gweon, S.Y. Zhou, J. Graf, C.M. Jozwiak, M.H. Jung, Y.S. Kwon, A. Lanzara, Phys. Rev. Lett. 98 (2007) 166403.
[16] N. Ru, R.A. Borzi, A. Rost, A.P. Mackenzie, J. Laverock, S.B. Dugdale, I.R. Fisher, Phys. Rev. B 78 (2008) 045123.
[17] K.Y. Shin, V. Brouet, N. Ru, Z.X. Shen, I.R. Fisher, Phys. Rev. B 72 (2005) 085132.
[18] M.D. Johannes, I.I. Mazin, Phys. Rev. B 77 (2008) 165135.
[19] K.Y. Shin, J. Laverock, Y.Q. Wu, C.L. Condron, M.F. Toney, S.B. Dugdale, M.J. Kramer, I.R. Fisher, Phys. Rev. B 77 (2008) 165101.
[20] C.D. Malliakas, M. Iavarone, J. Fedor, M. Kanatzidis, J. Am. Chem. Soc. 130 (2008) 3310.
[21] F. Pfuner, L. Degiorgi, K.Y. Shin, I.R. Fisher, Eur. Phys. J. B 63 (2008) 11–16.
[22] E. DiMasi, B. Foran, M.C. Aronson, S. Lee, Chem. Mater. 6 (1994) (1867).
[23] N.P. Ong, P. Monceau, Phys. Rev. B 16 (1977) 3443.
[24] J.A. Wilson, Phys. Rev. B 19 (1979) 6456.
[25] N. Shima, J. Phys. Soc. Jpn. 51 (1982) 11.
[26] F. Devreux, J. Phys. (Paris) 43 (1982) 1489.
[27] M. Nunez Regueiro, J.-M. Mignot, D. Castello, Europhys. Lett. 18 (1992) 53.